Journal of Dermatological Science 93 (2019) 14–23

Contents lists available at ScienceDirect

Journal of Dermatological Science

journal homepage: www.jdsjournal.com

Original Article

Cell-to-cell transmission of HSV-1 in differentiated keratinocytes promotes multinucleated giant cell formation

Yoshiko Yamamoto[a], Takenobu Yamamoto[a,b,*], Yumi Aoyama[a], Wataru Fujimoto[a]

[a] Department of Dermatology, Kawasaki Medical School, 577 Matsushima, Kurashiki 701-0192, Japan
[b] Department of Dermatology, Kawasaki Medical School, General Medical Center, 2-6-1 Nakasange, Kita-ku, Okayama 700-8505, Japan

ARTICLE INFO

Article history:
Received 26 June 2018
Received in revised form 29 August 2018
Accepted 12 September 2018

Keywords:
Herpes simplex virus
Keratinocyte
Differentiation
Multinucleated giant cell
Cell-to-cell fusion
Cell-to-cell transmission

ABSTRACT

Background: Herpes simplex virus (HSV) infection in the skin causes small grouped vesicles characterized by acantholytic cells and multinucleated giant cells (MGCs). Although viral factors have been studied as fusion proteins, little is known how the differentiation status of keratinocytes is involved in the formation of MGCs by HSV-1 infection.
Objective: As the human epidermis is composed of several layers of keratinocytes that undergo terminal differentiation, we aimed to elucidate whether the differentiation status of keratinocytes affects viral entry, propagation, cell-to-cell transmission of HSV-1, and MGC formation.
Methods: HaCaT cells and normal human epidermal keratinocytes were cultured in either low- or high-Ca^{2+} medium. After HSV-1 infection, cellular morphology, viral propagation, and expression of cytoskeletal and intercellular adhesion molecules were examined sequentially. Viral entry, replication, and expression of HSV receptors were analyzed. Cell-to-cell transmission and fusion after HSV-1 infection was evaluated using the Cell Tracker™ Red CMTPX dye system.
Results: Keratinocytes in high-Ca^{2+} medium formed MGCs, but those in low-Ca^{2+} medium formed single nuclear round cells in response to HSV-1 infection. HSV-1 entered the keratinocytes more effectively in low-Ca^{2+} than in high-Ca^{2+} medium, although transcripts of HSV receptors were comparable in both conditions. HSV-1 could replicate more efficiently in high-Ca^{2+} than in low-Ca^{2+} medium. A cell-to-cell fusion assay showed that HSV-1-infected and adjacent-uninfected keratinocytes were involved in MGCs in high-Ca^{2+} but not in low-Ca^{2+} medium.
Conclusion: Differentiated keratinocytes promote MGC formation by cell-to-cell fusion with resolution of cell membrane and cell-to-cell transmission of HSV-1 from infected keratinocytes to neighboring uninfected keratinocytes.

1. Introduction

The herpes simplex viruses (HSVs) are neurotropic and epidermotropic viruses that cause a wide range of clinical disorders with primary and recurrent infections. A disseminated HSV-1 infection of the skin, eczema herpeticum, is commonly seen in patients with atopic dermatitis, suggesting impaired barrier function and dysregulated immune response in these patients [1,2].

Clinically, multinucleated giant cells (MGCs) detected by a Tzanck smear of scrapings from early lesions have been known to be a diagnostic clue of HSV infection. The histopathology of HSV infection shows intraepidermal vesicle with ballooning degeneration of keratinocytes (KCs), acantholytic cells (ACs), and MGCs. As enveloped viruses, HSV-1 must fuse their envelope with the membrane of KCs to initiate infection. Although viral factors such as viral envelope glycoprotein B (gB) and gD have been extensively studied as fusion proteins [3,4], little is known whether differentiation status of KCs affect the formation of MGCs in response to epidermal HSV-1 infection.

The human epidermis is a multi-layered self-renewing sheet of KCs that undergo terminal differentiation and play an important role in barrier function [5]. A recent *ex-vivo* infection study using murine epidermis showed HSV-1 initially invaded the basal layer

Abbreviations: AC, acantholytic cell; DAPI, 4',6-Diamidino-2-phenylindole, dihydrochloride; Dsc, Desmocollin; Dsg, Desmoglein; Dsp, Desmoplakin; EDGS, EpiLife Defined Growth Supplement; gB, glycoprotein B; HSV, herpes simplex virus; HVEM, herpesvirus entry mediator A; KC, keratinocyte; MGC, multinucleated giant cell; MOI, multiplicity of infection; NHEK, normal human epidermal keratinocyte; NMHC-II, nonmuscle myosin heavy chain II; PBS, phosphate-buffered saline; pfu, plaque forming unit; poi, post of infection; RT-PCR, reverse transcriptional polymerase chain reaction.

* Corresponding author at: Department of Dermatology, Kawasaki Medical School, 577 Matsushima, Kurashiki City, Okayama, 701-0192, Japan.
E-mail address: go-yama@med.kawasaki-m.ac.jp (T. Yamamoto).

https://doi.org/10.1016/j.jdermsci.2018.09.006
0923-1811/

of undifferentiated epidermal cells and spread to the suprabasal layers [6,7]. These studies indicate that the differentiation of KCs has some regulatory roles in HSV entry and propagation.

Entry of HSV into cells depends upon multiple cell surface receptors and multiple proteins on the surface of the virion. The virion envelope gD receptors for HSV-1 include (i) HVEM (herpesvirus entry mediator), (ii) nectin-1 and nectin-2, and (iii) specific sites on heparan sulfate generated by certain 3-O-sulfotransferases [8]. Currently, nonmuscle myosin heavy chain IIA (NMHC-IIA) and IIB (NMHC-IIB) was identified as novel HSV-1 entry coreceptors that associate with gB [9].

To clarify the role of the differentiation status of KCs on susceptibility to HSV-1 entry, propagation, and formation of MGCs in human epidermal KCs, we performed experiments on HSV-1 infection in cultured HaCaT cells and normal human epidermal keratinocytes (NHEKs) with different extra-cellular calcium conditions.

Here, we showed that HSV-1 entry was more efficient in undifferentiated KCs cultured in low-Ca^{2+} medium, but formation of MGCs in response to HSV-1 infection was promoted in differentiated KCs cultured in high-Ca^{2+} medium. In the epidermis, it is thought that HSV-1 first enters target KCs and propagates in a manner of cell-to-cell transmission by direct fusion at the plasma membrane. Cell-to-cell fusion assays, which we established to evaluate HSV-1 cell-to-cell transmission and fusion with resolution of cell membrane *in vitro*, further confirmed that MGCs were efficiently formed in differentiated KCs cultured in high-Ca^{2+} medium.

2. Materials and methods

2.1. Cell line and Cell culture

The immortalized human keratinocyte HaCaT cells purchased from CLS Cell Lines Service, Eppelheim, Germany, were maintained in EpiLife medium (Thermo Fisher Scientific, Waltham, MA) supplemented with 0.03 mM Ca^{2+} (low-Ca^{2+}), then switched to high-Ca^{2+} medium with 2.8 mM Ca^{2+} in order to induce differentiation [10].

NHEKs were obtained from Thermo Fisher Scientific and maintained in EpiLife medium containing 0.06 mM Ca^{2+} (low-Ca^{2+}), then switched to high-Ca^{2+} with 1.2 mM Ca^{2+}.

2.2. Virus and infection

Wild-type HSV-1 (KOS strain) was obtained from the Research Institute for Microbial Diseases, Osaka University. HaCaT cells and NHEKs at 90% confluency were infected with HSV-1 at several multiplicity of infection (MOI) and incubated for 1 h at 37 °C to allow virus adsorption. The culture medium was then replaced with newly prepared medium containing 5 mg/mL of human γ-globulin (Gammagard, Baxter Healthcare, West Village, CA) to limit the spread of the virus to surrounding cells [11].

2.3. Measurement of virus replication

HSV-1 replication was measured by the plaque assay as described in supplement Materials and Methods.

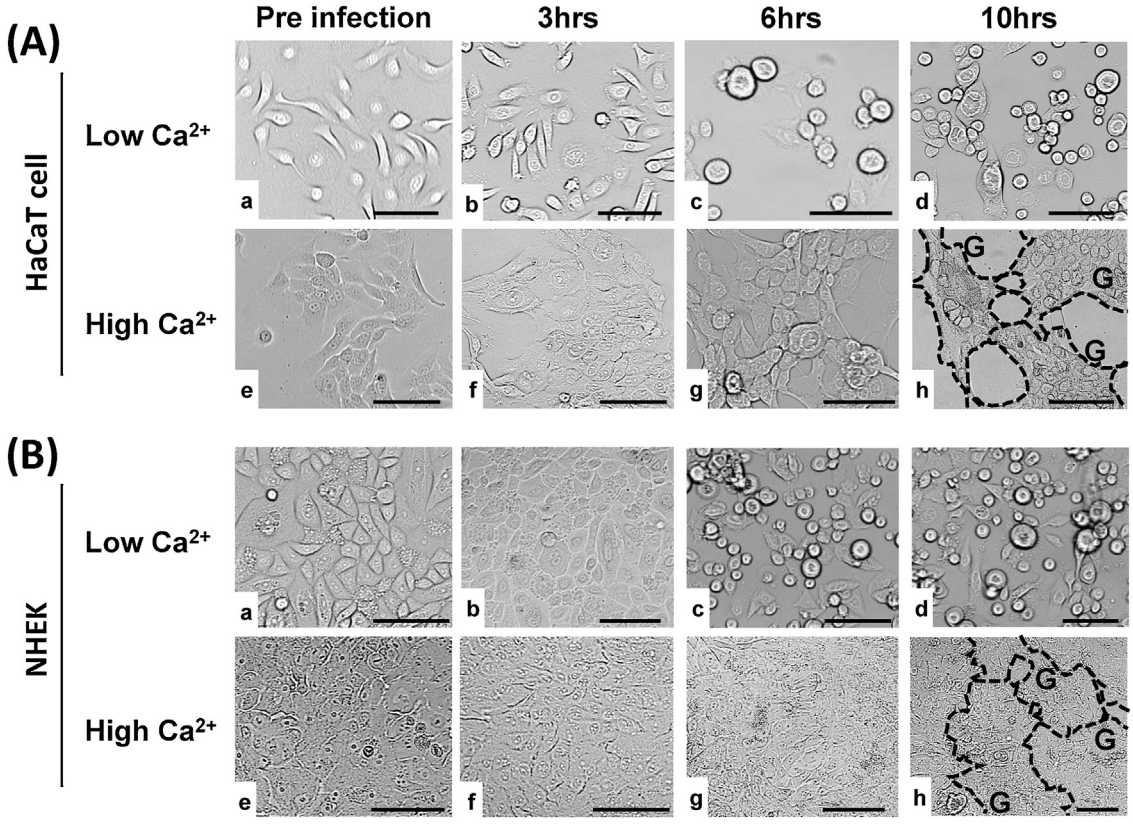

Fig. 1. Morphological change of KCs with HSV-1 infection by bright-field microscopy.
The form of KCs changed from unicellular spindle or round shape in low-Ca^{2+} medium to polygonal shape and sheet-like formation in high-Ca^{2+} medium. MGCs is formed with HSV-1 infected KCs cultured in high-Ca^{2+} but not in low-Ca^{2+} medium.
A: HaCaT cells; B: NHEKs; a-d: cultured in low-Ca^{2+} medium; e-h: cultured in high-Ca^{2+} medium.
a, e: before HSV-1 infection; b, f: 3 h poi; c, g: 6 h poi; d, h: 10 h poi.
G: multinucleated giant cell; Bar = 100 μm.

2.4. Quantitative RT-PCR

Quantitative RT-PCR was performed with the StepOnePlusTM Real-Time PCR System (Thermo Fisher Scientific). Protocols and specific primer sets are indicated in supplement Materials and Methods.

2.5. Transmission Electron microscopy

Virus propagation and cellular morphological changes were studied by electron microscopy as described in supplement Materials and Methods.

2.6. Immunofluorescence and immunoblot analysis

HaCaT cells and NHEKs infected with HSV-1 were used for immunofluorescence and immunoblot analysis. Protocols and antibodies were indicated in supplement Materials and Methods.

2.7. Cell-to-Cell fusion assays

Cell Tracker™ Red CMPTX Dye system (Thermo Fischer Scientific) was used for the detection of cell-to-cell fusion by exchange of cytoplasmic fluorescent dye. Protocols were indicated in supplement Materials and Methods.

2.8. Fluorescent microscopy of viral entry

The efficiency of HSV-1 entry was calculated as described in supplement Materials and Methods.

2.9. Statistics

Analyses were performed using SPSS for Windows version 20.0 (SPSS). A Mann-Whitney U test was used to compare the categorical variables. P-values of < 0.05 were considered significant.

3. Results

3.1. KCs in high-Ca^{2+} medium form MGCs, but those in low-Ca^{2+} medium form single nuclear round cells in response to HSV-1 infection

Morphological changes to KCs were observed sequentially by bright-field. KCs with low-Ca^{2+} medium showed a spindle shape. By switching low-Ca^{2+} to high-Ca^{2+} medium for a 48 h-incubation, KCs showed a polygonal shape and sheet-like formation (Fig. 1-a, e).

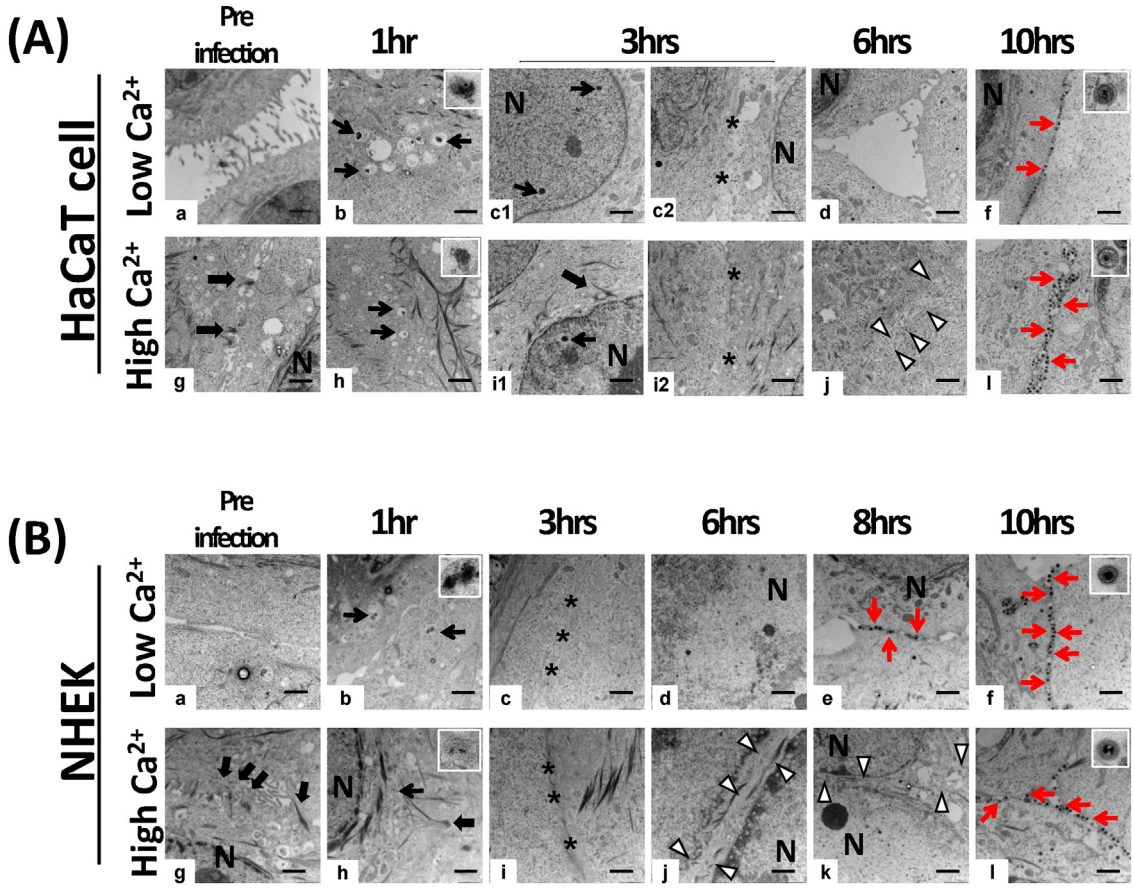

Fig. 2. Morphological change associated with HSV-1 infection in KCs by electron microscopy.
(A) HaCaT cells: Viral particles (black arrow) were seen in the cytoplasm and nucleus at 1 and 3 h poi, respectively. New replicated particles (red arrow) were detected in the intercellular space at 10 h poi.
(B) NHEKs: Viral particles (black arrow) were seen in the cytoplasm at 1 h poi. New replicated particles (red arrow) were detected in the intercellular space at 8 and 10 h poi in both low- and high-Ca^{2+} medium.
(A, B) HSV-1 infected cells showed narrowing of the intercellular gap (asterisk) after 3 h poi in both low- and high-Ca^{2+} medium. A portion of the cytoplasmic membrane dissapeared (triangle in *j*, k) after 6 h poi of KCs kept in high-Ca^{2+} medium, but not in low-Ca^{2+} medium. The desmosomal structures (large arrow in g, h, i1) were seen in the cellular membrane in high-Ca^{2+} medium.
a-f: cultured in low-Ca^{2+} medium; g-l: cultured in high-Ca^{2+} medium.
a, g: before HSV-1 infection; b, h: 1 h poi; c, i: 3 h poi; d, *j*: 6 h poi; e, k: 8 h poi; f, l: 10 h poi.
N: Nucleus; Bar = 1 μm.

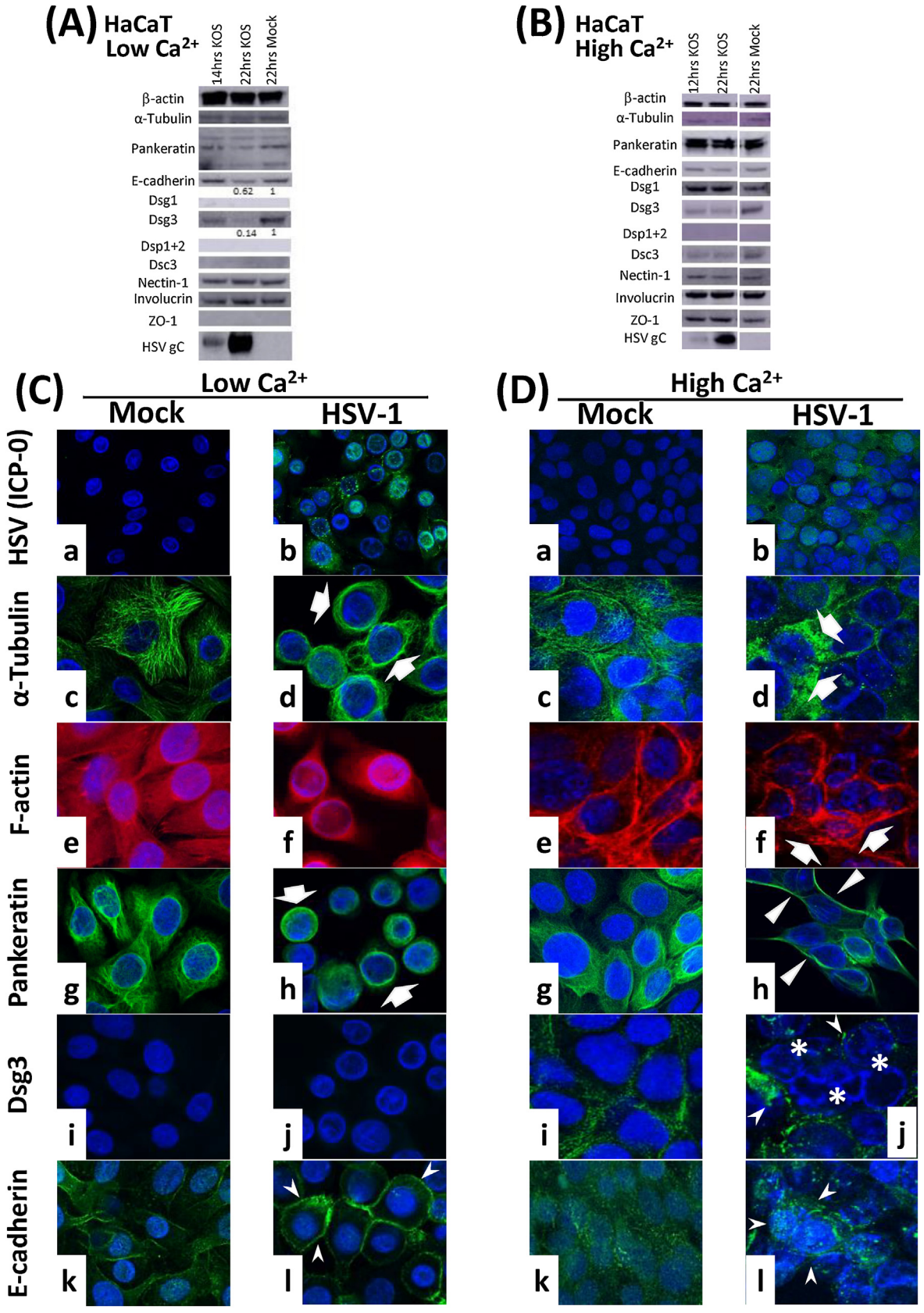

Fig. 3. Protein analysis.
(A, B) Stable expression level of the cytoskeletal and intercellular adhesion proteins in HaCaT cells after HSV-1 infection.
Expression level of cytoskeletal proteins including β-actin, α-tubulin, and pankeratin and intercellular adhesion proteins including Dsg 1, Dsc 3, Nectin-1, and ZO-1 in HSV-1 infected HaCaT cells were almost equivalent to those in the mock condition even after 12 or 14 and 22 h poi. Expression of E-cadherin and Dsg 3 in HSV-1 infected cells in low-Ca^{2+} medium was apparently reduced compared with those in the mock condition. HSV gC that belongs to HSV late gene was used to check HSV-1 infection.
(C, D) Distribution of cytoskeletal filaments and intercellular adhesion molecules in HaCaT cells in low- or high-Ca^{2+} medium after HSV-1 infection.

Involucrin, Desmoglein 1 (Dsg 1), Keratin 1, and *Keratin 10* mRNA transcripts were up-regulated in KCs by high-Ca^{2+} treatment for 48 h. On the other hand, *Keratin 5* and *Keratin 14* mRNA were down-regulated (supplement Fig.). These data indicated that differentiation of HaCaT cells and NHEKs was induced by switching from low-Ca^{2+} to high-Ca^{2+} medium, as described previously [12–14]. Differentiated KCs induced by incubation in high-Ca^{2+} medium for at least 48 h were used for further analyses.

HSV-1 or the mock condition was inoculated onto HaCaT cells and NHEKs incubated in either low- or high-Ca^{2+} medium at an MOI of 1 to check the unicellular morphological change. The form of HSV-1-infected HaCaT cells and NHEKs in low-Ca^{2+} medium changed from a spindle to round shape at 3 h post of infection (poi) and sustained the round shape at 6 h poi, whereas mock-infected HaCaT cells and NHEKs remained spindle-shaped, respectively. Interestingly, MGCs were never observed in HSV-1-infected HaCaT cells and NHEKs in low-Ca^{2+} medium at 10 h poi (Fig. 1 a–d). On the other hand, HSV-1-infected HaCaT cells and NHEKs in high-Ca^{2+} medium migrated to make an aggregated form at 6 h poi and showed MGCs at 10 h poi (Fig. 1e–h), whereas mock-infected HaCaT cells and NHEKs retained only sheet-like growth, respectively. These data indicate that the formation of MGCs induced by HSV-1 infection depends on extracellular Ca^{2+} concentration, namely differentiation status of KCs. In contrast, HSV-1-infected KCs remained in a “round” shape and did not regain a “spindle” shape when maintained in low-Ca^{2+} medium, namely undifferentiation status of KCs.

3.2. Similar distribution of viral particles but distinct morphological changes to HSV-1-infected KCs by transmission electron microscopy

HaCaT cells and NHEKs were inoculated with HSV-1 in low- or high-Ca^{2+} medium at an MOI of 1 and incubated for 1 h at 37 °C to allow virus adsorption. HaCaT cells and NHEKs were fixed pre-infection and at 1, 3, 6, 8, and 10 h poi.

Before HSV-1 infection, the desmosomal structures in the intercellular space were observed in HaCaT cells and NHEKs in high-Ca^{2+} medium, but they were not observed in those cells in low-Ca^{2+} medium (Fig. 2-a, g). Viral particles were detected in the cytoplasm of HaCaT cells and NHEKs at 1 h poi in both low- and high-Ca^{2+} medium (Fig. 2-b, h), and they were present in the nuclei at 3 h poi in low- and high-Ca^{2+} medium (Fig. 2A-c1, i1). Newly reproduced viral particles in HaCaT cells and NHEKs were detected in the intercellular space at 8 or 10 h poi in both low- and high-Ca^{2+} medium (Fig. 2A, B).

HSV-1-infected HaCaT cells and NHEKs showed narrowing of the intercellular gap at 3 h poi in both low- and high-Ca^{2+} medium, as compared with mock-infected cells (Fig. 2-c, i). In high Ca^{2+} medium, however, a portion of the cytoplasmic membrane in HSV-1-infected HaCaT cells and NHEKs disappeared and the desmosomal structures were abolished at the site of the intercellular gap narrowing at 6 h poi (Fig. 2-*j*). These data indicate that HSV-1 infection induced narrowing of the intercellular gap within 3 h poi and newly replicated virions were released from the cellular membrane within 8-10 h poi in both undifferentiated and differentiated KCs. But only in differentiated KCs, cell-to-cell fusion with resolution of cell membrane can occur at 6 h poi, suggesting possible syncytial formation.

3.3. Protein analyses

3.3.1. Stable expression level of the cytoskeletal and intercellular adhesion proteins after HSV-1 infection

HaCaT cells in low- and high-Ca^{2+} medium were infected with HSV-1 at an MOI of 0.05 or the mock condition for 12 or 14 and 22 h. Low titer of HSV-1 was used because HSV-1 infected KCs inoculated with high titer of HSV-1 and cultured for a long time should be easily detached from the flask. The expression levels of cytoskeletal proteins including β-actin, α-tubulin, and pankeratin in HSV-1-infected HaCaT cells were almost equivalent to those in the mock group even after 12 or 14 and 22 h poi. The expression levels of intercellular adhesion proteins including Dsg 1, Desmoplakin 1&2 (Dsp 1 + 2), Desmocollin 3 (Dsc 3), Nectin-1, Involucrin, and ZO-1 in HSV-1 infected cells were also equivalent to those in the mock group (Fig. 3A, B). E-cadherin and Dsg 3 in HSV-1-infected cells in low-Ca^{2+} medium were slightly reduced compared with those in the mock group (Fig. 3A). These data indicate that KCs change their morphology dramatically but maintain the level of expression of cytoskeletal and intercellular adhesion proteins for at least 22 h after HSV-1 infection. It is possible that reduction of the E-cadherin and Dsg 3 Levels in HSV-1-infected cells in low-Ca^{2+} medium is due to unknown direct HSV-1 effect or a short biological half-life of these proteins.

3.3.2. Altered distribution of cytoskeletal and intercellular adhesion proteins in response to HSV-1 infection

HaCaT cells were cultured in low- and high-Ca^{2+} medium and infected with HSV-1 at an MOI of 0.05 or the mock condition. Cells were fixed at 22 h poi and stained for these structural proteins and ICP-0 with DAPI. Almost all cells were positive for ICP-0 after HSV-1 infection, whereas no ICP-0-positive cells were detected under mock conditions in low- and high-Ca^{2+} medium at 22 h poi (Fig. 3C, D-a, b). Three kinds of cytoskeletal filaments, F-actin, α-tubulin, and pankeratin, showed fine fibrillar structures in the cytoplasm under mock conditions in low- and high-Ca^{2+} medium (Fig. 3C, D-c, e, g). After HSV-1 infection, these cytoskeletal filaments created a thin lamellar structure close to the nuclear membrane in low-Ca^{2+} medium (Fig. 3C-d, f, h). On the other hand, fine fibrillary structures of α-tubulin and F-actin transformed to a granular pattern, and pankeratin showed a streamlined shape in the cytoplasm in high-Ca^{2+} medium after HSV-1 infection (Fig. 3D-d, f, h).

In mock-infected cells, Dsg 3 was not detected in low-Ca^{2+} medium but was expressed as fine dots in the cytoplasm in high-Ca^{2+} medium (Fig. 3C, D-i). After HSV-1 infection, the expression of Dsg 3 was abolished and instead localized at the cell periphery as a coarse granular pattern (Fig. 3D-j). In mock-infected cells, E-cadherin was expressed as faint dots in the intercellular space and/or cytoplasm in both low- and high-Ca^{2+} medium (Fig. 3C, D-k). Upon HSV-1 infection, distribution of E-cadherin in low-Ca^{2+} medium was distinct at the cell periphery or in the intercellular space (Fig. 3C-l), whereas in high-Ca^{2+} medium the distribution was a coarse granular pattern mainly at the cell periphery (Fig. 3D-l). These data indicate that infection with HSV-1 drastically altered distribution of cytoskeletal filaments and intracellular adhesion molecules.

HaCaT cells were cultured in low-Ca^{2+} **(C)** or high-Ca^{2+} medium **(D)** and infected with HSV-1 or the mock condition for 22 h. Mock (a, c, e, g, i, k) and HSV-1 infected (b, d, f, h, j, l) cells were fixed and stained with ICP-0 (*green*, a, b), α-Tubulin (*green*, c, d), F-actin (*red*, e, f), pankeratin (*green*, g, h), Dsg 3 (*green*, i, j), E-cadherin (*green*, k, l), and DAPI (*blue*, a–l).
(**C**) α-Tubulin, F-actin, and pankeratin showed lamellar formation close to the nuclear membrane (large arrow) in the cytoplasm with HSV-1 infection. E-cadherin showed coarse granular formation (white arrow) in the intercellular space with HSV-1 infection.
(**D**) α-tubulin and F-actin showed granular formation (large arrow) and pankeratin showed streamlined shape (triangle) in the cytoplasm with HSV-1 infection. Dsg 3 tended to be lacked at crowded with the nucleus (asterisk), and Dsg 3 and E-cadherin showed coarse granular formation (white arrow) in the intercellular space with HSV-1 infection.

3.4. HSV-1 can enter the KCs more effectively in low-Ca^{2+} medium but replicate more effectively in high-Ca^{2+} medium

3.4.1. HSV-1 entry detected by ICP-0 staining

Successful HSV-1 entry was visualized by staining with an antibody against the viral immediate-early protein ICP-0. The cellular localization of ICP-0 passes through distinct phases during early infection; ICP-0 in nuclear foci indicates an early stage of viral gene expression, which is followed by the relocalization of ICP-0 to the cytoplasm [15,16].

HaCaT cells and NHEKs in low- and high-Ca^{2+} medium were inoculated with HSV-1 at an MOI of 0.5 to evaluate the efficiency of HSV1 entry adequately. HSV-1-inoculated cells were fixed and permeabilized at 45 and 60 min poi. The fixed cells were stained with ICP-0 and DAPI. The level of HSV-1 inoculation to the KCs was calculated by determining the ratio of the number of ICP-0-positive cells in the nuclei to that of the DAPI-positive cells. At least three independent spots per one sample were calculated, and the efficiency of HSV-1 entry was statistically compared with two conditions: low- and high-Ca^{2+} medium.

In HaCaT cells, 21.3% and 8.32% of ICP-0-stained cells were detected in low- and high-Ca^{2+} medium at 60 min poi, respectively (Fig. 4-a, c). In NHEKs, 16.0% and 4.08% of ICP-0-stained cells were detected in low- and high-Ca^{2+} medium at 60 min poi, respectively (Fig. 4-b, d). These data indicate that entry of HSV-1 in KCs were more efficient in low-Ca^{2+} than in high-Ca^{2+} medium.

3.4.2. Comparable expression of HSV receptor mRNA in undifferentiated and differentiated KCs

We analyzed and compared the level of HSV receptor expression in KCs under both conditions. Expression of HSV-1 entry receptor transcripts: *Nectin-1*, *HVEM*, *NMHC-IIA (hMYH9)*, and *NMHC-IIB (hMYH10)*, tended to decrease in HaCaT cells in high-Ca^{2+} medium, but they did not differ significantly between the two conditions except for expression of *NMHC-IIA (hMYH9)* mRNA that was down-regulated in high-Ca^{2+} medium (Fig. 4-e). The expression levels of these receptors in NHEKs maintained in high-Ca^{2+} medium were equivalent to those in low-Ca^{2+} medium (Fig. 4-f). These results indicate that efficiency of HSV-1 entry does not depend only on entry receptors examined.

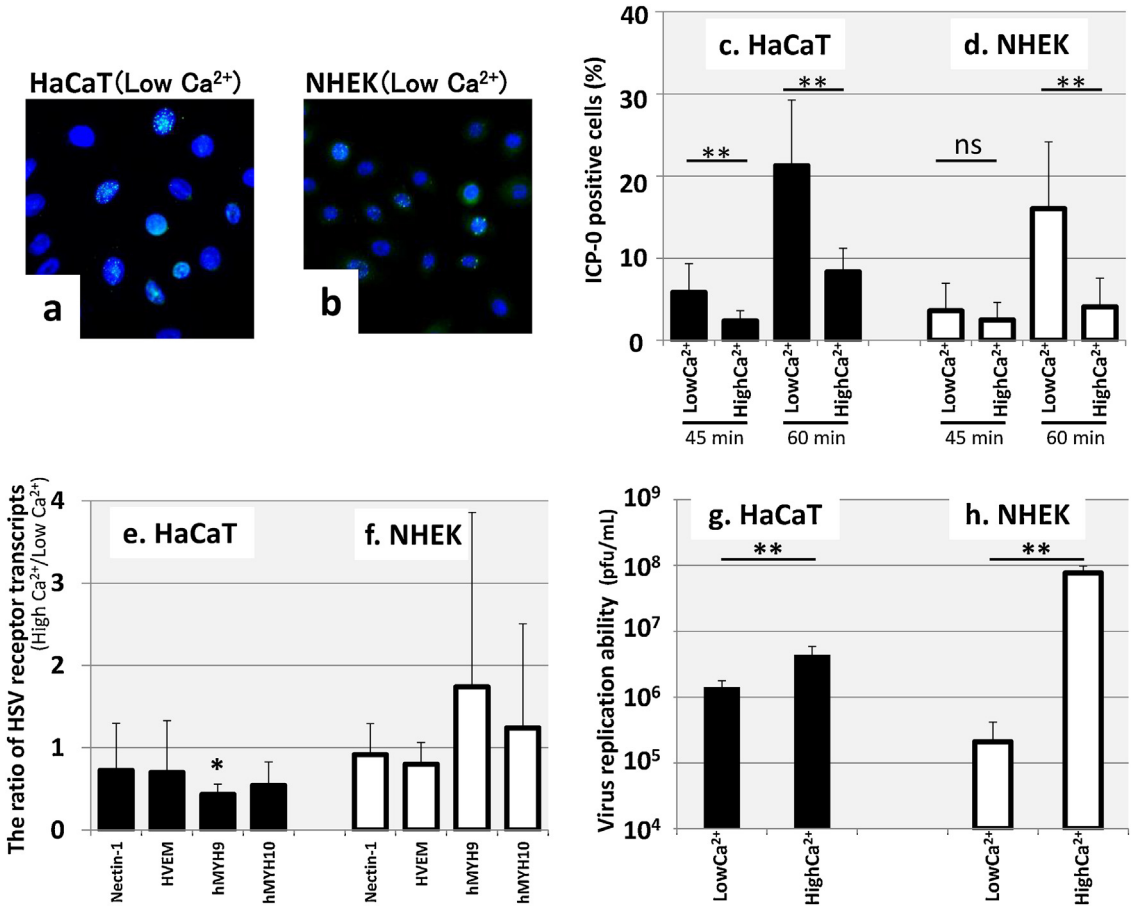

Fig. 4. HSV-1 can enter the KCs more effectively in low-Ca^{2+} but replicate more effectively in high-Ca^{2+} medium.
HSV-1 inoculated HaCaT cells (a) and NHEKs (b) in low-Ca^{2+} medium were stained with anti-ICP-0 (green) and DAPI (blue) at 60 min poi.
The ratio of ICP-0 positive HaCaT cells (c) and NHEKs (d) in the nuclei was indicated. HSV-1 can enter KCs within 60 min more easily in low-Ca^{2+} than in high-Ca^{2+} medium, significantly (c, d).
The ratio of HSV receptor transcripts of HaCaT cells (e) and NHEKs (f) in high-Ca^{2+} to those in low-Ca^{2+} medium; *Nectin-1*, *HVEM*, and *NMHC-IIA*, *-IIB (hMYH9, 10)* were calculated. HSV receptor transcripts tended to decrease in HaCaT cells in high-Ca^{2+} medium but did not differ significantly between two conditions except for expression of *NMHC-IIA (hMYH9)* (e). *NMHC-IIA*, *-IIB* mRNAs tended to increase in NHEKs in high-Ca^{2+} medium but did not differ significantly between two conditions (f).
HSV-1 can replicate more effectively in high-Ca^{2+} than in low-Ca^{2+} medium (g, h).
g: HaCaT cells, h: NHEKs.
Numbers are mean ± SD of at least triplicate experiments.
**: $p < 0.01$, *: $p < 0.05$, *ns*: not significant with Mann-Whitney *U* test.

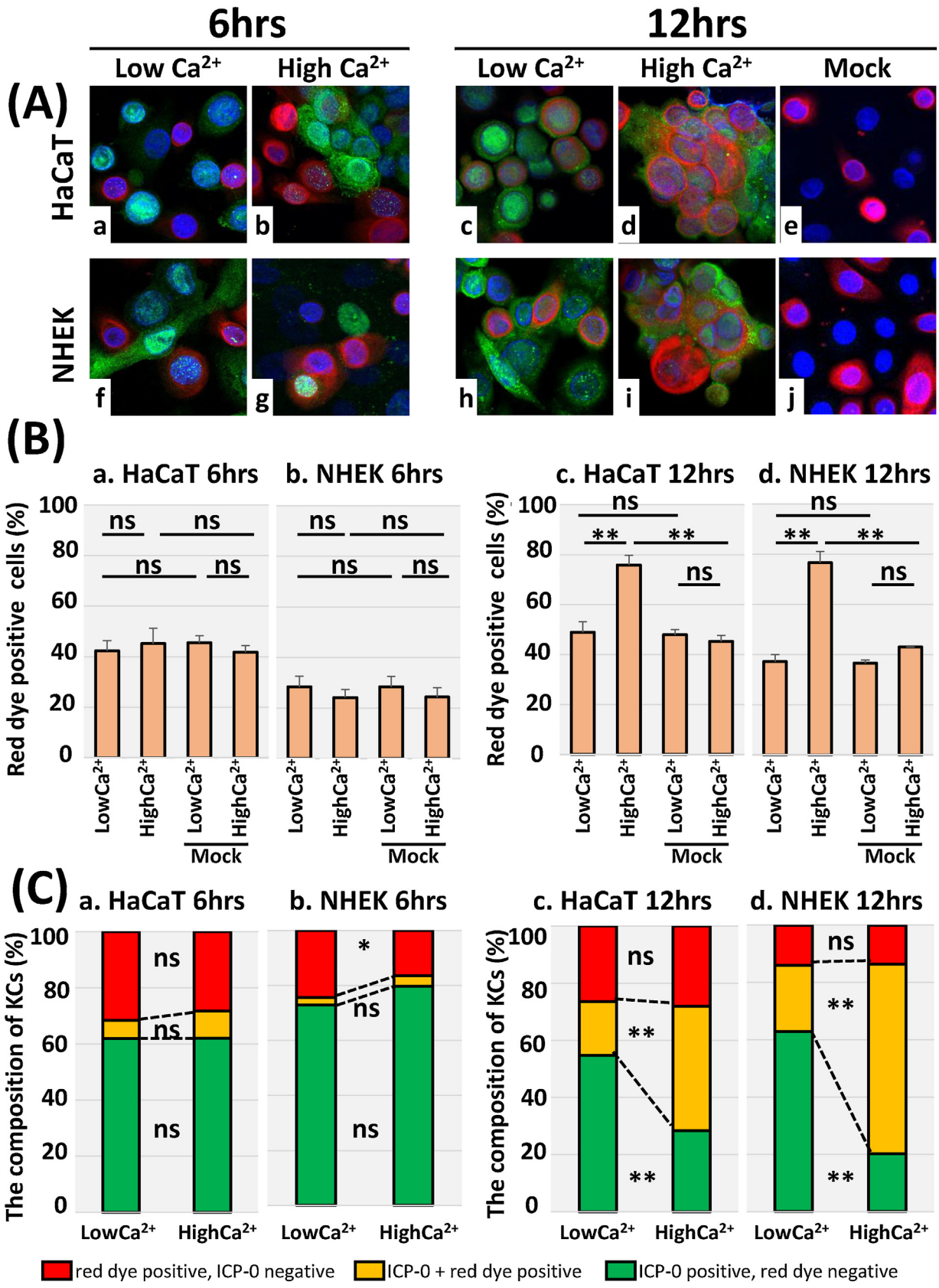

Fig. 5. Propagation of HSV-1 infection by cell-to-cell transmission and MGCs formation in differentiated KCs.
(A) Numerous target KCs showed ICP-0 positive (reddish purple cytoplasm with orange rim and light blue nuclei) which were adjacent to HSV-1 infected effector KCs (green color in the cytoplasm or nuclei) in low-Ca^{2+} medium (a, c, f, h). MGCs consist of ICP-0 positive effector KCs (green cytoplasm with blue nuclei) and ICP-0 positive target KCs (reddish purple cytoplasm with orange rim, and light blue nuclei) in high-Ca^{2+} medium for 12 h co-cultivation (d, i). Mock infected condition did not show any orange or green colored cells (e, j).
a-e: HaCaT cells; f-j: NHEKs; a, c, e, f, h, j: cultured in low-Ca^{2+} medium; b, d, g, i: cultured in high-Ca^{2+} medium; e, j: target KCs were co-cultivated with mock infected effector KCs.

3.4.3. HSV-1 can replicate more effectively in high-Ca^{2+} than in low-Ca^{2+} medium

HaCaT cells and NHEKs were inoculated with HSV-1 at an MOI of 0.05 in low- and high-Ca^{2+} medium. Cells were collected at 22 h poi and cell-free virus was purified. Replicated HSV-1 virions were measured by a viral plaque assay. HSV-1 growth in HaCaT cells with low- and high-Ca^{2+} medium showed 1.42×10^6 and 4.40×10^6 plaque forming unit (pfu)/mL, respectively (Fig. 4-g). HSV-1 growth in NHEKs with low- and high-Ca^{2+} medium showed 2.10×10^5 and 7.65×10^7 pfu/mL, respectively (Fig. 4-h). These data indicate that HSV-1 growth is significantly increased in high-Ca^{2+} medium compared with low-Ca^{2+} medium.

3.5. Propagation of HSV-1 infection by cell-to-cell transmission and MGCs formation in differentiated KCs

In vivo, HSV-1 infects cells through initial attachment and subsequent fusion of the virion envelope with the plasma membrane or through contiguous cell-to-cell spread by a not yet understood mechanism [17]. We established a novel assay system to evaluate cell-to-cell transmission from HSV-1-infected KCs to non-infected KCs *in vitro*. Non-infected detached target KCs labeled with Cell Tracker™ Red CMPTX Dye were transferred to and co-cultivated with the adherent HSV-1-infected effector KCs for either 6 or 12 h. Cell Tracker™ Red CMTPX dye is transferred to daughter cells and retained in living cells through several generations. The red dye does not migrate to adjacent cells in a population but should be expanded to other cells when cell-to-cell fusion with resolution of cell membrane is induced [18,19]. The co-cultivated cells were stained with ICP-0 (green) and DAPI (blue). Target KCs should show red color in the cytoplasm and blue color in the nuclei. HSV-1-infected ICP-0-expressing effector KCs should show green color in the cytoplasm or blue color with light blue spots in the nuclei. Although effector KCs were prepared with inoculation of HSV-1 at an MOI of 5 to make all effector KCs infected, a part of effector KCs was uninfected with HSV-1 which should show blue color in the nuclei without cytoplasmic green color.

The red-colored cells in the cytoplasm occupied 36.6–48.0% of DAPI-positive cells in mock-infected HaCaT cells and NHEKs in both low- and high-Ca^{2+} medium after 12 h of co-cultivation, indicating mononuclear cells derived from non-infected target KCs (Fig. 5A-e, *j* and B-c, d). After 12 h co-cultivation of the effector and target KCs, there were numerous orange-colored cells in the cytoplasm adjacent to HSV-1 infected effector KCs in HaCaT cells and NHEKs in low-Ca^{2+} medium (Fig. 5A-c, h). These cells indicated newly infected cells derived from non-infected target KCs by cell-to-cell transmission without resolution of cell membrane, and they were observed together with some light blue-colored cells in the nuclei with red color in the cytoplasm, probably indicating an early stage of newly infected target KCs before the relocalization of ICP-0 in cytoplasm after 12 h of co-cultivation. Notably, we could not find any MGCs in HaCaT cells and NHEKs in low-Ca^{2+} medium. In contrast, there were a lot of MGCs in HaCaT cells and NHEKs in high-Ca^{2+} medium that consisted of several colored cells including red, green, and orange color in the cytoplasm as well as blue, green, and light blue color in the nuclei after 12 h of co-cultivation (Fig. 5A-d, i).

Since red dye is an indicator of cell division or cell-to-cell fusion with resolution of cell membrane of target KCs, we counted the number of red dye-positive cells, namely red or orange colored cells, ICP-0 expressing green cells, and DAPI (blue) in low- and high-Ca^{2+} media. The ratio of the number of the red dye-positive cells to that of the DAPI-positive cells was calculated by counting at least three independent spots per one sample. The rate of red dye-positive cells did not differ regardless of extracellular calcium conditions in both HaCaT cells and NHEKs after 6 h of co-cultivation (Fig. 5B-a, b). After 12 h of co-cultivation with mock-infected HaCaT cells, the red dye-positive cells were 48.0% and 45.3% in low- and high-Ca^{2+} medium, respectively. Co-cultivation with HSV-1-infected HaCaT cells, however, the red dye-positive cells were 48.9% in low Ca^{2+} medium but 76.0% in high-Ca^{2+} medium (Fig. 5B-c). Similarly, after 12 h co-cultivation with mock-infected NHEKs, the red dye-positive cells were 36.6% and 43.1% in low- and high-Ca^{2+} medium, respectively. Co-cultivation with HSV-1-infected NHEKs, on the contrary, the red dye-positive cells were 37.3% in low-Ca^{2+} medium but 76.6% in high-Ca^{2+} medium after 12 h of co-cultivation (Fig. 5B-d). Thus, it revealed that the ratio of the red dye-positive cells was significantly higher in high-Ca^{2+} medium compared with those in low-Ca^{2+} medium for 12 h of co-cultivation with HSV-1-infected HaCaT cells and NHEKs. These results suggest that cell division or cell-to-cell fusion with resolution of cell membrane took place in differentiated KCs but not in undifferentiated KCs.

KCs were divided into three kinds of phase on this cell-to-cell fusion assays: red colored target KCs without HSV-1 infection, green colored effector KCs with HSV-1 infection (red dye negative), and KCs showing orange or comprised with both colors. The distribution among three kinds of KC was unchanged compared with low- and high-Ca^{2+} medium condition after 6 h co-cultivation (Fig. 5C-a, b). However, after 12 h co-cultivation, the rate of the green colored effector KCs with HSV-1 infection (red dye negative) was reduced and that of KCs showing orange or both colors was increased in high-Ca^{2+} medium condition (Fig. 5C-c, d). These data indicate that in high Ca^{2+} medium, a part of effector KCs takes Cell Tracker™ Red CMTPX dye by cell-to-cell fusion with target KCs. Taken together, these results indicate that HSV-1 can propagate from target KCs to neighboring uninfected KCs in a manner of cell-to-cell transmission without resolution of cell membrane up to 6 h co-cultivation regardless of the extracellular calcium condition. However, during 6-12 h co-cultivation, along with HSV-1 propagation, cell-to-cell fusion with resolution of KCs cell membrane takes place and results in the formation of MGCs in differentiated KCs.

4. Discussion

Our present work has three major findings concerning MGC formation in two differentiation states of KCs. First, differentiated KCs in high-Ca^{2+} medium form MGCs, but undifferentiated KCs in low-Ca^{2+} medium form single nuclear round cells by HSV-1 infection. Second, HSV-1 can enter more effectively in undifferentiated KCs than in differentiated KCs, whereas HSV-1 can replicate more efficiently in opposite KCs. Third, HSV-1-infected and adjacent uninfected KCs are involved in MGC formation *via* cell-to-cell fusion with resolution of cell membrane and cell-to-cell

(B) The ratio of the red dye positive cell showed much higher in co-cultivation with HSV-1 infected HaCaT cells and NHEKs in high-Ca^{2+} medium than those with low-Ca^{2+} medium or mock infected KCs for 12 h co-cultivation.
The ratio of the red dye positive cell to DAPI positive cell; a: for 6 h co-cultivation in HaCaT cells, b: for 6 h co-cultivation in NHEKs, c: for 12 h co-cultivation in HaCaT cells, d: for 12 h co-cultivation in NHEKs.
(C) The distribution among three kinds of KC was unchanged compared with low- and high-Ca^{2+} medium after 6 h co-cultivation. The rate of the green colored effector KCs with HSV-1 infection (red dye negative) was reduced and that of KCs showing orange or both red and green colors was increased in high-Ca^{2+} medium after 12 h co-cultivation.
Numbers are mean ± SD of at least triplicate spots.
**: $p < 0.01$, *ns*: not significant with Mann-Whitney *U* test.

transmission of HSV-1 in differentiated KCs but not in undifferentiated KCs.

Using the well-established and simple system of monolayer culture of two KCs, we first confirmed that the narrowing of the intercellular gap occurred in both undifferentiated and differentiated KCs at 3 h poi when viral capsids were already present in nucleus but before the appearance of newly reproduced viral particles in the intercellular space at 8-10 h poi (Fig. 2). Narrowing of the intercellular gap after HSV-1 infection might lead to increased efficiency of cell-to-cell transmission by keeping Nectin-1 expression [17], which was maintained for at least 22 h after HSV-1 infection in both low- and high-Ca^{2+} medium (Fig. 3A, B). However, our results indicate that the narrowing of intercellular gap of KCs in the early stage of HSV-1 infection is not induced by newly replicated viral envelope as a "glue" of cell membranes of adjacent KCs. Although newly reproduced viral particles were detected in intercellular space of both undifferentiated and differentiated KCs at 8-10 h, cell-to-cell fusion with the resolution of cell membranes and subsequent formation of MGCs were detected only in differentiated KCs at 10 h poi (Fig. 1). Taken together, the attachment of cell membranes is induced by HSV-1 infection in both undifferentiated and differentiated KCs, but MGC formation requires cell-to-cell fusion with resolution of cell membrane.

By the viral immediate-early protein ICP-0 staining [15,16], we confirmed that HSV-1 can enter the KCs more effectively in undifferentiated KCs grown in low-Ca^{2+} medium than in differentiated KCs in high-Ca^{2+} medium (Fig. 4a–d). Quantitative RT-PCR revealed that *nectin-1* and *HVEM* (cellular receptors of gD) and *NMHC-IIA* and *-IIB* (cellular receptors of gB) are not down-regulated convincingly by differentiation, although expression of *NMHC-IIA (hMYH9)* mRNA was slightly down-regulated in high-Ca^{2+} medium (Fig. 4e, f). These results indicate that efficiency of HSV-1 entry does not depend only on entry receptors examined in this study. Higher efficiency of HSV-1 entry in undifferentiated KCs may depends on factors aside from HSV-1 receptors, including glycosaminoglycan chains of cell surface proteoglycans to which HSV-1 bind at initial contact before binding to entry receptors [8]. Or it depends on the difference of cytoplasmic events between undifferentiated and differentiated KCs after binding of HSV-1 to its receptors. In contrast to the HSV-1 entry, replication of HSV-1 is increased in differentiated KCs compared with undifferentiated KCs (Fig. 4-g, h). The reason is not clear, but it might suggest that HSV-1 takes advantage of available cellular machineries for replication more in differentiated KCs. Taken together, our data suggest that HSV-1 might be able to enter the undifferentiated basal-like KCs more effectively but then replicate efficiently in the differentiated form of the spinous to granular layer-phase KCs.

In contrast to simultaneous, direct HSV-1 contact to each KCs *in vitro*, HSV-1 infection starts with entry into particular cells and proceeds in a manner of cell-to-cell transmission *in vivo*. To clarify whether the formation of MGC is also reproduced in a manner of cell-to-cell transmission *in vitro*, we established a novel assay using "The Cell Tracker™ Red CMTPX fluorescent dye". In this assay, cell-to-cell transmission can be evaluated accurately because human γ-globulin is added in medium in order to limit the spread of the cell-free virus to surrounding cells [11]. Also, the assay has an advantage that cell division or cell fusion can be determined.

First, since the rate of the red dye-positive cells showed no difference in co-cultivation with either mock or HSV-1 infected KCs in low-Ca^{2+} condition (Fig. 5B), it was assumed that HSV-1 spread to the adjacent HSV-1 non-infected target KCs *via* cell-to-cell transmission without resolution of cell membrane in low-Ca^{2+} condition. Second, although either cell division or cell-to-cell fusion with resolution of cell membrane was suggested to occur in differentiated KCs but not in undifferentiated KCs after 12 h co-cultivation, further analyses of red cells (ICP-0 negative), green cells (ICP-0 positive) and cells comprised with both colors showed a convincing evidence that a part of effector KCs takes Cell Tracker™ Red CMTPX dye by cell-to-cell fusion with target, differentiated but not undifferentiated KCs (Fig. 5C). In other word, HSV-1 takes unidirectional spread from the effector KCs to target KCs by cell-to-cell transmission in both undifferentiated and differentiated KCs. However, in differentiated KCs, infection of HSV-1 is bidirectional in that HSV-1 spread from effector KC to target KCs and then these infected target KCs make cell-to-cell fusion with effector KCs resulting in MGC formation. Increase of red dye positive cells in HaCaT cells could be due in part by cell division, because HaCaT cells were more proliferative in high-Ca^{2+} compared with low-Ca^{2+} medium [20]. However, increase of red dye positive cells in NHEK as well makes this assumption less possible, because the addition of calcium induces decreased proliferation in NHEKs.

This report has some limitations. Direct influence of Ca^{2+} induced cell-cell attachment and intercellular interaction on MGC formation could not be excluded. We used non-syncytial KOS strain in this assay because HSV-1 KOS strain is one of the most frequently analyzed strains. It would be interesting whether syncytial HSV-1 strains such as ANGpath or KOS syn also results in MGC formation or viral replication in the similar manner as observed in our study.

Conflict of interest

The authors have no conflict of interest to declare.

Funding

This work was supported by Research Project Grants (26-038, 27-059, 28-091, and 29-043) from Kawasaki Medical School.

Acknowledgements

We thank Ms. Yoko Yoshida, Mr. Yoshitaro Itano, and Mr. Nobuaki Matsuda for the helpful discussion and comments on quantitative RT-PCR and ultrastructural technique.

Appendix A. Supplementary data

Supplementary material related to this article can be found, in the online version, at doi:https://doi.org/10.1016/j.jdermsci.2018.09.006.

References

[1] P.S. Gao, N.M. Rafaels, T. Hand, T. Murray, M. Boguniewicz, T. Hata, et al., Filaggrin mutations that confer risk of atopic dermatitis confer greater risk for eczema herpeticum, J. Allergy Clin. Immunol. 124 (2009) 507–513.
[2] A.D. Benedetto, M.K. Slifka, N.M. Rafaels, I.H. Kuo, S.N. Georas, M. Boguniewicz, et al., Reductions in claudin-1 may enhance susceptibility to herpes simplex virus 1 infections in atopic dermatitis, J. Allergy Clin. Immunol. 128 (2011) 242–246.
[3] J. Fontana, D. Atanasiu, W.T. Saw, J.R. Gallagher, R.G. Cox, J.C. Whitbeck, et al., The fusion loops of the initial prefusion conformation of herpes simplex virus 1 fusion protein point toward the membrane, Mbio 8 (2017) e01268–17.
[4] H.B. Rogalin, E.E. Heldwein, Interplay between the herpes simplex virus 1 gB cytodomain and the gH cytotail during cell-cell fusion, J. Virol. 89 (2015) 12262–12272.
[5] E. Proksch, J.M. Brandner, J.M. Jensen, The skin: an indispensable barrier, Exp. Dermatol. 17 (2008) 1063–1072.
[6] E. Rahn, P. Petermann, K. Thier, W. Bloch, J. Morgner, S.A. Wickstrom, et al., Invasion of herpes simplex virus type 1 into murine epidermis: an ex vivo infection study, J. Invest. Dermatol. 135 (2015) 3009–3016.
[7] P. Petermann, K. Thier, E. Rahn, F.J. Rixon, W. Bloch, S. Ozcelik, et al., Entry mechanisms of herpes simplex virus 1 into murine epidermis: involvement of nectin-1 and herpesvirus entry mediator as cellular receptors, J. Virol. 89 (2015) 262–274.
[8] P.G. Spear, Herpes simplex virus: receptors and ligands for cell entry, Cell Microbiol. 6 (2004) 401–410.

[9] J. Arii, Y. Hirohata, A. Kato, Y. Kawaguchi, Nonmuscle myosin heavy chain IIb mediates herpes simplex virus 1 entry, J. Virol. 89 (2015) 1879–1888.
[10] A.F. Deyrieux, V.G. Wilson, In vitro culture conditions to study keratinocyte differentiation using the HaCaT cell line, Cytotechnology 54 (2007) 77–83.
[11] P. Tebas, E.C. Stabell, P.D. Olivo, Antiviral susceptibility testing with a cell line which expresses beta-galactosidase after infection with herpes simplex virus, Antimicrob. Agents Chemother. 39 (1995) 1287–1291.
[12] J. Woodcock-Mitchell, R. Eichner, W.G. Nelson, T.T. Sun, Immunolocalization of keratin polypeptides in human epidermis using monoclonal antibodies, J. Cell Biol. 95 (1982) 580–588.
[13] M. Regnier, P. Vaigot, M. Darmon, M. Prunieras, Onset of epidermal differentiation in rapidly proliferating basal keratinocytes, J. Invest. Dermatol. 87 (1986) 472–476.
[14] R.L. Eckert, M.B. Yaffe, J.F. Crish, S. Murthy, E.A. Rorke, J.F. Welter, Involucrin-structure and role in envelope assembly, J. Investig. Dermatol. Symp. Proc. 100 (1993) 613–617.
[15] P. Petermann, I. Haase, D. Knebel-Morsdorf, Impact of Rac1 and Cdc42 signaling during early herpes simplex virus type 1 infection of keratinocytes, J. Virol. 83 (2009) 9759–9772.
[16] P. Petermann, E. Rahn, K. Thier, M.J. Hsu, F.J. Rixon, S.J. Kopp, et al., Role of nectin-1 and herpesvirus entry mediator as cellular receptors for herpes simplex virus 1 on primary murine dermal fibroblasts, J. Virol. 89 (2015) 9407–9416.
[17] F. Cocchi, L. Menotti, P. Dubreuil, M. Lopez, G. Campadelli-Fiume, Cell-to-cell spread of wild-type herpes simplex virus type 1, but not of syncytial strains, is mediated by the immunoglobulin-like receptors that mediate virion entry, Nectin1 (PRR1/HveC/HIgR) and Nectin2 (PRR2/HveB), J. Virol. 74 (2000) 3909–3917.
[18] S. Bär, M. Alizon, Role of the ectodomain of the gp41 transmembrane envelope protein of human immunodeficiency virus type 1 in late steps of the membrane fusion process, J. Virol. 78 (2004) 811–820.
[19] S. Bär, A. Takada, Y. Kawaoka, M. Alizon, Detection of cell-cell fusion mediated by Ebola virus glycoproteins, J. Virol. 80 (2006) 2815–2822.
[20] L. Micallef, F. Belaubre, A. Pinon, C. Jayat-Vignoles, C. Delage, M. Charveron, et al., Effects of extracellular calcium on the growth-differentiation switch in immortalized keratinocyte HaCaT cells compared with normal human keratinocytes, Exp. Dermatol. 18 (2009) 143–151.